Journal of Materials Chemistry B

PAPER

View Article Online
View Journal | View Issue

Cite this: J. Mater. Chem. B, 2018, 6, 7503

Synergic TiO_2 photocatalysis and guanine photoreduction for silver deposition amplification: an ultrasensitive and high-throughput visualized colorimetric analysis strategy for anthrax DNAs in blood using a wettable microwells array

Huan Liu, Luping Feng, Yuanyuan Cai, Yue Hua, Min Liu, Mengyuan Yin, Shuai Li, Xiaoxia Lv, Jiangwei Wen and Hua Wang *

Received 23rd September 2018,
Accepted 8th October 2018

DOI: 10.1039/c8tb02500b

rsc.li/materials-b

An ultrasensitive and high-throughput visualized colorimetric method has been initially developed with a wettable microwells array for probing guanine base-containing anthrax DNAs in blood based on silver deposition amplified by the synergic TiO_2 photocatalysis and guanine photoreduction under visible light. Hydrophilic microwells were first created on the hydrophobic slides to yield the wettable microwells array, on which photocatalytic titanium dioxide (TiO_2) nanoparticles were deposited with dopamine (DA) to yield TiO_2@DA for anchoring single strand DNA (ssDNA) capture probes without guanine bases. After the hybridization of the targeted anthrax DNAs, exonuclease I (Exo I) was introduced into the microwells to selectively digest the unhybridized ssDNA probes. The silver deposition was further conducted by the synergic photocatalysis of TiO_2@DA and photoreduction of guanine bases of anthrax DNAs, thus achieving the amplified silver signals for the visualized colorimetric assays. Moreover, benefitting from the wettability feature of the hydrophilic–hydrophobic interfaces of the microwells array so fabricated, DNA analytes could be accumulated from the sample droplets through the condensing enrichment process to realize the ultrasensitive detection, in addition to circumventing any crossover contaminants between the sample droplets. The developed visualized colorimetric method with the microwells array was subsequently applied for probing anthrax DNAs in blood with levels down to 1.0 fM. DNAs with single-base and double-base mutations could also be identified accurately. Importantly, such a biosensing design route of a wettable microwells array, in combination with the photocatalytic silver deposition and specific Exo I-catalytic probe digestion, may promise extensive applications for the high-throughput, ultrasensitive, and selective detection of guanine-containing DNA targets with ultra-trace levels in complicated samples like blood.

Introduction

Anthrax as a bacterial disease caused by *Bacillus anthracis* can seriously affect animals and humans.[1,2] In particular, anthrax attack with *Bacillus anthracis* as a bioterrorism agent has attracted increasing concerns because of its high mortality in humans and animals.[3–6] Therefore, exploring a rapid, selective, and high-throughput detection method for anthrax is of crucial importance for the clinical diagnosis and bioterrorism prevention of anthrax disease. It is well recognized that the quantification of anthrax DNAs in the blood is thought to be an efficient and reliable way for monitoring anthrax.[7–10] For example, Zhang and his co-workers reported a colorimetric detection method for probing anthrax DNAs.[9] Our group also developed a magnetic separation-based detection method for the electroanalysis of anthrax DNAs using a gold-mineralized enzyme.[10]

Moreover, the diagnosis and screening of diseases may involve the analysis of multiple biomarkers and/or samples. However, most of the common methods may encounter problems with high-throughput analysis. As a result, many efforts have been devoted to the development of microarrays or chips for the high-throughput analysis of biomarkers like DNAs of importance.[8,11–16] For example, Gao's group has established a high-throughput microarray for detecting the circulating miRNAs in human serum.[13] Yet, most of the testing microarrays can suffer from the

Institute of Medicine and Materials Applied Technologies, College of Chemistry and Chemical Engineering, Qufu Normal University, Qufu, 273165, P. R. China.
E-mail: huawang@qfnu.edu.cn; Web: http://wang.qfnu.edu.cn;
Fax: +86 5374456306; Tel: +86 5374456306

crossover contaminations in-between the sample droplets of complex media like blood, making it difficult to fabricate dense testing dots for the multiple analysis of samples.[17] In addition, the catalytic silver deposition route has been widely applied as a signal amplification route for the detection of various nucleic acids.[18–21] For example, Nam *et al.* reported a chip-based detection method for targeting anthrax DNAs in the form of bar-code DNAs through the gold catalytic silver deposition.[8] Zhou and colleagues reported a biomineralization-assisted amplification methodology by silver deposition for the sensitive detection of DNAs.[18]

In the present study, an ultrasensitive and high-throughput colorimetric strategy has been proposed for the detection of anthrax DNAs containing guanine bases, based on silver deposition amplified by the synergic TiO_2 photocatalysis and guanine photoreduction. Herein, TiO_2 nanomaterials, which are photocatalysts generally applied in solar cells and cleanup of toxic organics,[22,23] were employed alternatively to photocatalyze the silver deposition on the targeting DNAs. The main detection principle and procedure are schematically illustrated in Scheme 1. Glass slides were first dotted with polyacrylic acid (PAA), and further patterned with hydrophobic hexadecyltrimethoxysilane (HDS). Then, NaOH was utilized to etch the PAA micro-dots to produce the hydrophilic microwells. Moreover, nano-scale TiO_2 particles were coated with dopamine (DA) into the microwells for covalently anchoring single-strand DNA (ssDNA) capture probes without guanine bases. After the hybridization of targeting anthrax DNAs containing guanine bases, exonuclease I (Exo I) was introduced to selectively digest the unhybridized ssDNA probes. The silver deposition was further performed by the synergic TiO_2 photocatalysis and photoreduction of guanine bases of anthrax DNAs, thus attaining the amplified silver signals for the visualized colorimetric assays. Remarkably, the wettability profile of the microwell arrays would additionally aid accumulation of more DNA analytes from the sample droplets *via* a condensing enrichment process. Any crossover contamination of the testing sample droplets may also be depressed to facilitate the selective analysis of targeting DNAs. Investigation results indicate that the developed analysis method could allow for the ultrasensitive and selective quantification of anthrax DNAs with low levels in blood including their mutant levels, showing the feasibility of being

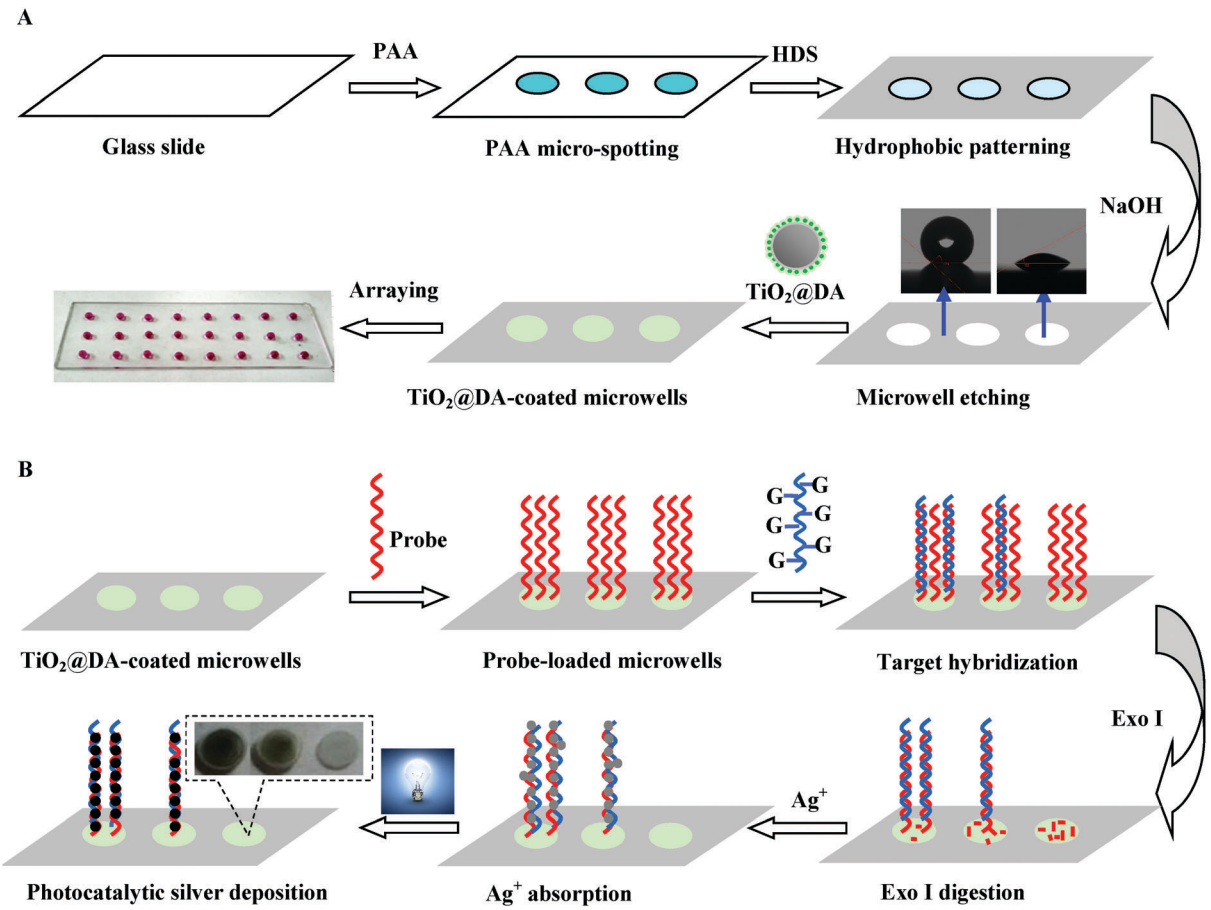

Scheme 1 Schematic illustrations of (A) the fabrication process of the wettable microwells array, including the PAA micro-spotting, hydrophobic HDS patterning, base etching, and TiO_2@DA coating, of which the as-prepared microwells array was exemplified using the water droplets of rhodamine B; (B) the detection principle and the procedure of the microwells array-based colorimetric assays for anthrax DNAs, including the probe cross-linking, target hybridization, Exo I digestion of unhybridized ssDNA probes, and photocatalytic silver deposition, showing the corresponding photographs of the silver products.

applied for the early diagnosis and the wide screening of exposure to anthrax.

Experimental section

Materials and instruments

Tetrabutyl titanate (TBOT), polyacrylic acid (PAA), polyethylene glycol (PEG), hexadecyl trimethoxysilane (HDS), cetyltrimethyl ammonium bromide (CTAB), and dithiothreitol (DTT) were obtained from Aladdin Reagent Co., Ltd (Shanghai, China). Silver nitrate ($AgNO_3$), rhodamine B, phosphate-buffered saline (PBS), glutaraldehyde, ethylenediaminetetraacetic acid (EDTA), tris(hydroxymethyl) aminomethane hydrochloride (Tris–HCl), and dopamine (DA) were purchased from Sinopharm Chemical Reagent Co. (China). Blood samples were kindly provided by the local university hospital. Deionized water (>18 MΩ, RNase-free) was supplied from an Ultra-pure water system (Pall, USA). Exonuclease I (Exo I), oligonucleotides of single-strand DNA (ssDNA) probes, anthrax DNAs containing guanine bases, single-base mutant and double-base mutant anthrax DNAs were synthesized by Sangon Biotech (Shanghai, China), with the base sequences including:

(1) DNA probe: 5′-ATC CTT ATC AAT ATT TAA CAA TAA TCC-3′;

(2) Wild anthrax DNA: 5′-GGA TTA TTG TTA AAT ATT GAT AAG GAT-3′;

(3) Single-base-mismatch anthrax DNA: 5′-GGA TGA TTG TTA AAT ATT GAT AAG GAT-3′;

(4) Double-base-mismatch anthrax DNA: 5′-GGA TGA TTG TTA CAT ATT GAT AAG GAT-3′.

Buffer solutions include the conjugation buffer (pH 7.2) containing 100 mM PBS and 150 mM NaCl; the hybridization buffer (pH 7.4) consisting of 10 mM Tris–HCl, 1.0 mM EDTA, 1.0 mM CTAB, and 100 mM NaCl; the DNA rinsing buffer (pH 7.4) composed of 50 mM NaCl and 10 mM Tris–HCl; Exo I buffer containing 67 mM glycine–KOH, 6.7 mM $MgCl_2$, and 10 mM DTT; and the silver deposition substrate consisting of 1.0 mM $AgNO_3$ and 2.0 mM $Mg(NO_3)_2$ in glycine buffer.

Blood samples were prepared by the protein precipitation route. Briefly, an aliquot of 500.0 μL of collected blood was vigorously mixed with 40.0 μL of 0.2 M HCl and 20.0 μL of 0.4 M PPh_3 (in water–acetonitrile 20 : 80 v/v and 2.0 M HCl). After incubation for 15 min, the hydrolysed blood was mixed with 500.0 μL of acetonitrile to precipitate proteins, followed by centrifugation at 4000 rpm for 20 min. The supernatant was used for further analysis.

The step-by-step fabrication of the microwells array was conducted with the wettabilities monitored by using a contact-angle measurement machine (Jinhe, Jiangsu, China). Transmission electron microscopy (TEM, JEM-2100PLUS, Japan) and inverted fluorescence microscopy (Olympus, IX73-DP80, Japan) were separately applied for the characterization of different materials or products. Moreover, field emission scanning electron microscopy (SEM, JSM-6700F, Japan) was employed to characterize the resulting surfaces of the TiO_2@DA deposited with silver. UV-3600 spectrophotometry (Shimadzu, Japan) was utilized to measure the UV-vis spectra of different functional materials such as TiO_2, TiO_2@DA and TiO_2@DA nanocomposites deposited with silver. Moreover, the absorbance intensities of deposited silver at 420 nm were colorimetrically measured using an Infinite M 200 PRO (TECAN, Switzerland), working with a home-made microplate holder adapted for the array tests. X-ray diffraction (XRD, Bruker D8 Advance) was utilized for exploring TiO_2@DA nanocomposites. The elemental mapping was conducted for the products using scanning electron microscopy (SEM, Hitachi E-1010, Horiba Ex-250) with a microanalysis system (EDAX, USA).

Preparation and characterization of TiO_2@DA nanocomposites

TiO_2 nanoparticles were fabricated by a sol–gel procedure with hydrothermal treatment. Typically, an aliquot of acetic acid (25 mL) was added into ethanol (20 mL) under vigorous stirring. Furthermore, an aliquot of TBOT (10 mL) in ethanol (20 mL) was dropped into the above mixture with the aid of an ultrasonicator, followed by the addition of PEG (0.70 g). Then, the resulting solution was transferred into a Teflon-lined stainless steel autoclave to be heated for 24 h at 160 °C. After the completion of the reaction, the mixture was cooled to room temperature, followed by washing three times separately with water and ethanol. Subsequently, the TiO_2 products were dried for 12 h at 60 °C, whose crystal structures were determined by the XRD with the detection range from 10 to 80 degrees.

An aliquot of 5.0 mg of the TiO_2 powder described above was added to 5.0 mL Tris–HCl buffer (pH 7.4) containing 12.5 mg DA to be mixed by sonication for 10 min, and then incubated overnight. After that, the so prepared DA-coated TiO_2 (TiO_2@DA) nanocomposites were washed with deionized water three times, and then diluted to 5.0 mL with Tris–HCl buffer and subsequently stored at 4 °C for future usage.

Fabrication of wettable microwells array

As schematically shown in Scheme 1A, the microwells array was fabricated using glass slides (72 mm × 24 mm) that were first cleaned with fresh piranha solution ($H_2SO_4 : H_2O_2 = 7 : 3$), then washed twice with water to be dried in nitrogen. Next, a 2 μL aliquot of PAA (10 mg mL^{-1}) was dotted onto the cleaned glass slides. Following that, those resulting slides were dipped into 5.0% HDS in ethanol for 2.0 h, and then dried in a vacuum. Further, an aliquot of NaOH (1.0 M) was dropped onto the slides to etch the PAA microdots to yield the wettable microwells array. The changing contact angles (CAs) of the interfaces of the microwells array so fabricated were monitored by the contact-angle measurements.

Microwells array-based colorimetric analysis for anthrax DNAs

Typically, an aliquot of TiO_2@DA (1.0 mg mL^{-1}) nanocomposites was first coated on the microwells. Then, an aliquot of 2.5% glutaraldehyde was introduced to activate the amino-derivatized TiO_2@DA for 40 min, followed by washing twice with Tris–HCl buffer. Furthermore, an aliquot of the amine-derivatized ssDNA capture probes (1.0 μM) was dropped into the microwells to be incubated for 1.0 h. Next, the hybridization buffers containing targeted anthrax DNAs with different

concentrations ranging from 0.0010 to 10.0 pM in buffer were separately added into microwells to conduct the hybridization reactions for 1.0 h at 37 °C, and then washed twice with the DNA rinsing buffer to remove any nonspecifically absorbed targets. After that, an aliquot of Exo I (0.50 U mL^{-1}) was introduced to be incubated at 37 °C for 30 min, followed by flushing twice separately with Exo I buffer and PBS to remove any unhybridized ssDNA probes or mismatched DNA sequences. Subsequently, the silver deposition substrate was added to be further exposed under visible light (100 W) for 5.0 min. The UV absorbance values of so yielded silver deposition products in microwells were measured at 420 nm.

According to the same procedure above, the microwells array-based colorimetric method was practically applied for probing wild anthrax DNAs with different concentrations spiked in blood. In addition, mutant-level identification experiments were conducted for the single-base mutant and double-base mutant anthrax DNAs spiked in the wild DNA samples at fixed total DNA concentrations of 1.0 pM.

Collection of blood samples

All the experiments were performed in compliance with the Ethical Committee Approval of China, and approved by the ethics committee at Qufu Normal University. Additionally, the blood samples were provided by the University Hospital at Qufu Normal University, which were collected from healthy volunteers with informed consent.

Results and discussion

Fabrication of wettable microwells array for the colorimetric analysis of anthrax DNAs by the photocatalytic silver deposition

The wettable microwells array was fabricated by following the procedure schematically illustrated in Scheme 1A. PAA was first spotted onto the cleaned glass substrates to be further patterned with the hydrophobic HDS layer. Furthermore, the spotted PAA microdots were etched using NaOH to yield the wettable microwells array, followed by the TiO_2@DA coatings. The step-by-step fabrication procedure was monitored by measuring the contact angles (CAs) of interfacial wettabilities, as detailed in Fig. 1. One can note from Fig. 1 that the average CAs of the yielded HDS patterns and microwell interfaces are about 137° and 19.9°, respectively. After being coated with TiO_2@DA, the resulting microwells could have a CA of about 29.9°. Remarkably, such a hydrophobic–hydrophilic wettability profile of the microwells array would help to accumulate the analytes from the sample droplets through a condensing enrichment process to realize more sensitive detections.[1,24] Additionally, the possible crossover contamination of testing sample droplets may be thus depressed to expect the selective analysis of targets. The so-yielded microwells array was further exemplified using rhodamine B droplets, which displays an excellent arraying performance. Besides, there are 24 microwells created on the array of glass slide (72 mm × 24 mm). Accordingly, it may allow for the detection of 24 samples in one experiment.

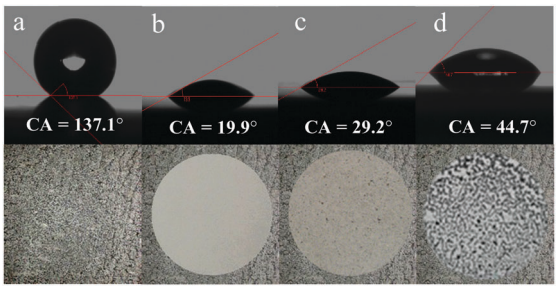

Fig. 1 The characterization for the microwells during the step-by-step fabrication and detection procedures after the (a) hydrophobic HDS patterning, (b) hydrophilic microwells substrate, (c) TiO_2@DA coating, and (d) the silver deposition photocatalyzed by TiO_2@DA after the DNA hybridizations, showing the corresponding changing CAs (top) and microscopy images (bottom).

Moreover, the main detection principle and procedure of the high-throughput microwells array for anthrax DNAs are schematically illustrated in Scheme 1B. As depicted in Scheme 1B, guanine base-containing DNA targets were captured by the ssDNA capture probes (without guanine bases) immobilized on the microwells through the hybridization reaction to form the double-stranded DNAs (dsDNAs). A selective digestion with Exo I was then conducted for the unhybridized ssDNA probes so as to ensure the specific analysis of DNA targets. Subsequently, Ag^+ ions were introduced into the testing microwells to conduct the silver deposition through the synergic TiO_2 photocatalysis and photoreduction of guanine bases of DNA targets under visible light.[20,21,25] Once the silver deposition was finished, the resulting microwells could be furnished with numerous silver particles together with an increased CA of about 44.7°, as topologically revealed in Fig. 1. Importantly, the resulting silver colorations could be rationally correlated to the concentrations of targeting DNAs towards the microwells array-based high-throughput analysis.

Characterization of the TiO_2@DA photocatalysts for the silver deposition towards the colorimetric assays for anthrax DNAs

The as-prepared TiO_2@DA coated in microwells before and after the silver deposition were characterized separately using powder X-ray diffraction (XRD) and UV-vis spectra, taking TiO_2 as the control (Fig. 2). One can note from Fig. 2A that TiO_2 nanoparticles could have the marked diffraction peaks of crystallinity in good agreement with the well established data

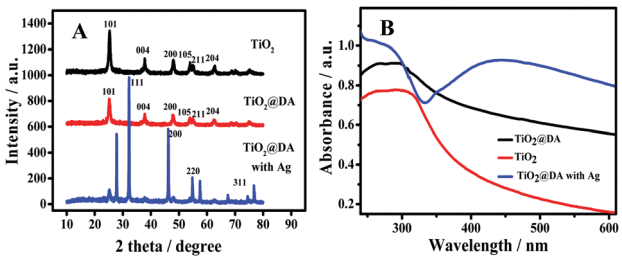

Fig. 2 Comparison of (A) XRD patterns and (B) UV-vis spectra among TiO_2, TiO_2@DA, and TiO_2@DA with deposited silver.

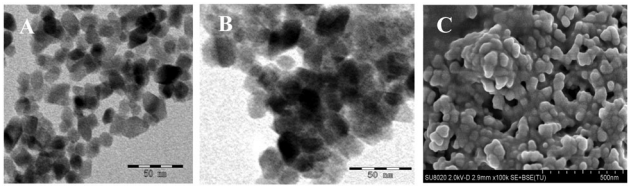

Fig. 3 (A) TEM image of TiO_2 nanoparticles and (B) TiO_2@DA nanocomposites. (C) SEM image of the surface of microwells coated with TiO_2@DA after the hybridization and the deposition of silver ions.

(JCPDS 72-1272), thus proving that the anatase-phase TiO_2 nanoparticles were synthesized. Also, these products can possess the diffraction peaks of TiO_2 at the same 2 Theta positions of anatase type, including 25.7° (101), 37.9° (004), 47.9° (200), 53.7° (105), 55.0° (211), and 62.9° (204). With the silver deposition after DNA hybridization, the resulting TiO_2@DA nanocomposites can display additionally the characteristic silver diffraction peaks like 32.2° (111), 45.5° (200), 67.5° (220), and 76.2° (311), which are basically consistent with Ag^0. Furthermore, the UV-vis spectra indicate that TiO_2 and TiO_2@DA both have the absorbance peak at 300 nm (Fig. 2B). After the silver deposition, as expected, the silver absorbance peak at 420 nm was observed, in addition to the TiO_2 one at 300 nm. One can note from Fig. 3A that TiO_2 nanoparticles were synthesized with well-defined particle structures, showing the average size of about 14 ± 2.1 nm in diameter (Fig. 3A). Also, most of the TiO_2@DA particles were clustered with an average size of about 17 ± 3.6 nm in diameter. Moreover, the topological structure of the TiO_2@DA coated in microwells with the silver deposition was characterized using scanning electron microscopy (SEM) (Fig. 3C). It was found that the TiO_2@DA with deposited silver could have a certain proportion of aggregation with the average size of about 60 ± 3.4 nm in diameter, in contrast to TiO_2 nanocatalysts that might display uniform mono-dispersion in water. Herein, the viscous DA as an enediol ligand can be tightly anchored onto TiO_2 nanocatalysts to enhance their photo-catalytic responses in the visible spectral region through adjusting the coordination geometry of Ti atoms on the TiO_2 surface,[20,26] so as to improve the photocatalysis for the silver deposition under visible light.

Besides, energy dispersive spectroscopy (EDS) was employed to explore the morphological structure and chemical composition of TiO_2@DA with deposited silver after the DNA targets hybridization. One can note from Fig. 4A that the products can possess a pretty high intensity of silver. In particular, the O, Ti, and Ag elements could be uniformly dispersed (Fig. 4B), thus confirming the elemental profile of TiO_2@DA after the silver deposition.

Sensing performances of the microwells array-based colorimetric method for anthrax DNAs by the photocatalytic silver deposition

The sensing performances of the microwells array-based colorimetric method for anthrax DNAs by the photocatalytic silver deposition were comparably investigated (Fig. 5). As shown in Fig. 5A, before the hybridization with the guanine

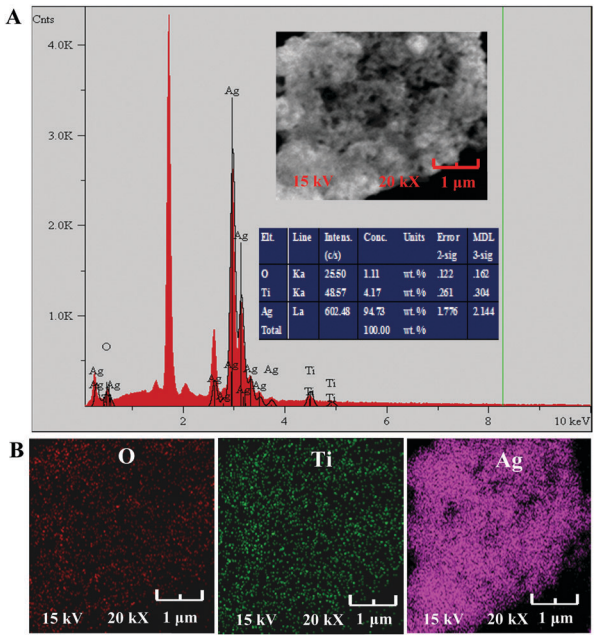

Fig. 4 (A) EDS spectra and (B) the element mapping (Ti, Ag, and O) of TiO_2@DA-coated microwells deposited with the silver products after the target hybridization and photocatalytic silver deposition reactions.

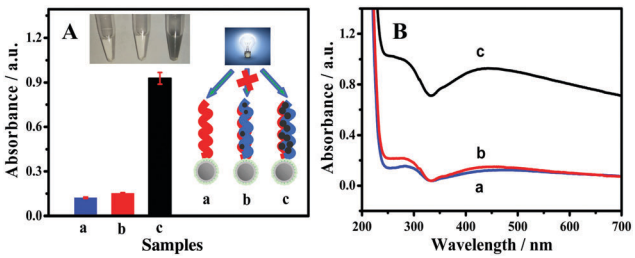

Fig. 5 (A) Comparison investigations on the colorimetric responses (inset: the photographs of the corresponding reaction products) and (B) UV-vis spectra of the products obtained by the TiO_2@DA-photocatalyzed silver deposition in the (b) absence and (c) presence of visible light after the hybridization of targeted anthrax DNAs (10.0 pM), taking (a) the TiO_2@DA-loaded probes alone as the control.

base-containing DNA targets, the silver deposition signal could be negligibly low for ssDNA probes without guanine bases, as evidenced by the silver absorbance. The ssDNA probes modified on TiO_2@DA would not significantly interact with silver ions to give the signal of silver deposition. It demonstrates that the silver deposition might hardly occur without photoreduction of the anthrax DNAs containing guanine bases. In addition, even though the ssDNA probes without silver-binding G bases might electrostatically adsorb silver ions, they could be removed from the testing area of the microwells by the Exo I-catalytic digestion, so that no silver deposition should occur there, thus ensuring the high analysis selectivity for targeted DNAs. Also, the silver deposition could not take place in the dark, thus confirming that the TiO_2@DA photocatalysis for the silver deposition should proceed under visible light, where DA coatings might enhance the photo-catalytic response

of TiO_2 in the visible spectral region so as to improve the photocatalytic silver deposition under visible light as aforementioned. The above facts can also be validated visually by the photographs of the corresponding product solutions of silver deposition (Fig. 5A, inset). Furthermore, Fig. 5B manifests the UV-vis spectra of the silver product solutions, confirming the silver deposition could be carried out through the synergic TiO_2 photocatalysis and guanine photoreduction. In addition, the so deposited silver products could have an apparent absorbance peak at 420 nm, which should be considered for the colorimetric detections for anthrax DNAs afterwards.

Main detection conditions of the microwells array-based colorimetric method for anthrax DNAs

The main detection conditions of the developed colorimetric method for anthrax DNAs were systematically optimized (Fig. 6). As shown in Fig. 6A, the colorimetric responses to anthrax DNAs could increase with the increasing TiO_2@DA concentrations till 0.80 mM, which should be selected for all colorimetric assays. Herein, too high TiO_2@DA concentrations might yield the coatings of TiO_2@DA photocatalysts with too high densities on the testing areas so as to negatively influence their photocatalysis for silver deposition resulting in the decreasing signals. Furthermore, Fig. 6B reveals that the coloration reactions of silver deposition could rely on the $AgNO_3$ concentrations, and the maximum coloration responses could be obtained at 50 mM $AgNO_3$, which should be selected as the optimal one. Also, the experimental investigations were performed on the photocatalysis time, with the data shown in Fig. 6C. One can see that the photocatalysis time could determine the coloration responses to anthrax DNAs, indicating that 6.0 min is sufficient for the photocatalysis. Moreover, the hybridization time for targeted DNAs was explored (Fig. 6D). Obviously, the coloration responses could increase as the hybridization time increased and tend to be steady after 50 min, which is thus chosen for the hybridization reactions. Fig. 6E describes that the colorimetric responses could change with the changing of the DNA capture probes concentrations, which reached the saturated state at 1.2 μM. Therefore, 1.2 μM of DNA capture probes is thereby selected for all of the colorimetric assays. Additionally, one can see from Fig. 6F that the targeting hybridization reactions can be pH-dependent with the coloration responses peak at pH 7, which is thereby selected as the optimal pH value in the hybridization experiments.

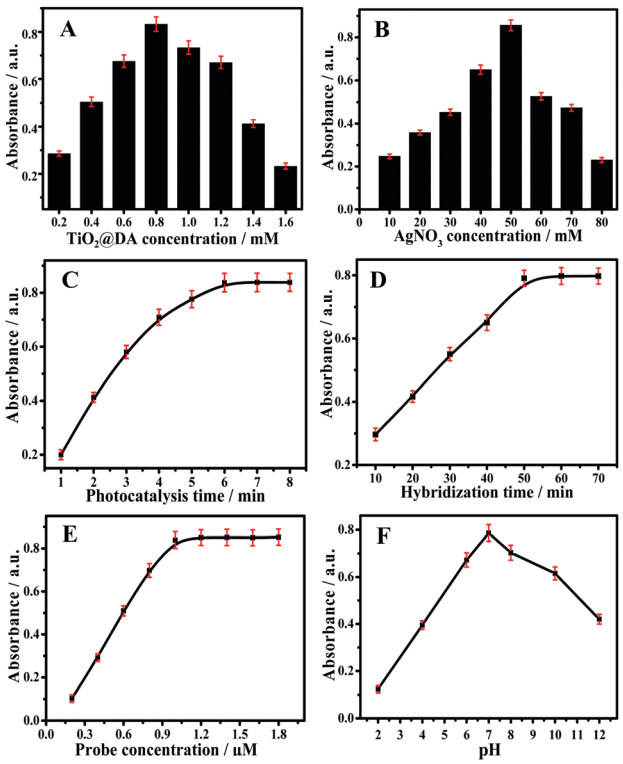

Fig. 6 Optimization of the main detection conditions for the microarray-based colorimetric assays for anthrax DNAs including (A) TiO_2@DA concentrations, (B) $AgNO_3$ concentrations, (C) illumination time, (D) DNA hybridization time, (E) capture probes concentrations, and (F) pH values. UV absorbance values of deposited silver products were recorded at a wavelength of 420 nm.

Preliminary applications of the microwells array-based colorimetric method for anthrax DNAs in samples

Under the optimized experimental conditions, the microwells array-based colorimetric detection method was employed to separately detect the wild anthrax DNAs and mutant ones (Fig. 7). Fig. 7A manifests the colorimetric responses to wild anthrax DNAs with different concentrations in buffer, with the photographs of the corresponding product droplets of silver

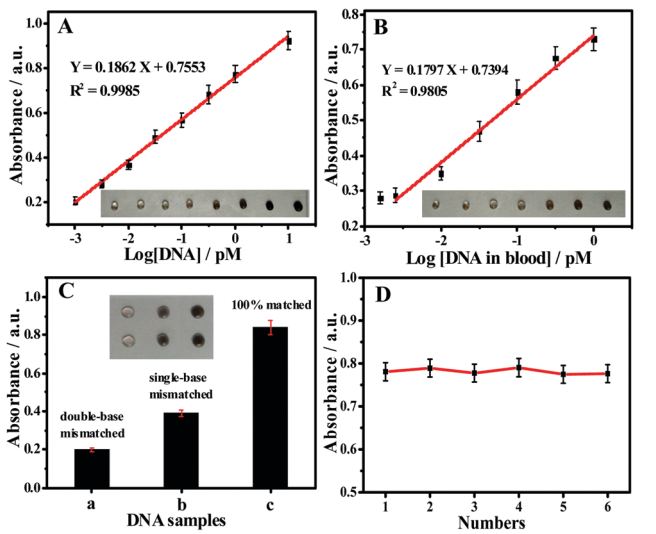

Fig. 7 The colorimetric calibration curves describing the relationships between absorbance changes and different concentrations of anthrax DNAs separately spiked in (A) buffer and (B) blood, with the corresponding photographs of the silver products photocatalytically deposited on the microwells array (inset). (C) Comparable identification among anthrax DNAs spiked in blood with (a) double-base mismatched, (b) single-base mismatched, and (c) matched sequences, with the corresponding photographs of the microwells array of three replicated experiments, where the absorbance values of the deposited silver products were recorded at 420 nm. (D) The reproducibility of the microwells array-based colorimetric method for the replicated detections of anthrax DNAs spiked in blood (1.0 pM).

deposition reactions (Fig. 7A, inset). A linear relationship was thus obtained for the colorimetric responses *versus* the logarithms of anthrax DNA concentrations ranging from 0.0010 to 10.0 pM (R^2 = 0.9985), with the detection limit of 0.25 fM estimated by the 3σ rule.

The developed visualized colorimetric analysis method was practically applied to evaluate the levels of wild DNA spiked in blood samples (Fig. 7B). A linear relationship was achieved for the product absorbance values *versus* the logarithms of anthrax DNAs concentrations in blood linearly ranging from 0.0025 to 1.0 pM (R^2 = 0.9805), with the detection limit of about 1.0 fM. Such a detection limit is much lower than those of most previous reports on the detections of anthrax DNAs like the ones of 1.0 pM[27] and 13 pM,[28] indicating that the developed colorimetric method can present favorable detection performances. Furthermore, Fig. 7C illustrates the comparison of identification among single-base mismatched DNAs, double-base mismatched DNAs, and matched DNAs, together with the photographs of the corresponding reaction product droplets. As expected, the single-base mismatched DNA showed lower responses than the matched ones, whereas the double-base mismatched DNAs could display the lowest responses. Accordingly, the as-developed colorimetric method enables the discrimination of mutation levels of single-base and double-base mismatched DNAs. Herein, the mutations of single and double guanine bases of DNAs might further decrease the guanine photoreduction abilities for the silver deposition to different degrees. The existence of mismatches in the DNA might additionally bring about an insulating barrier to prevent the hole migration to the guanine-guanine accepting sites thus leading to a decrease in the TiO_2 photocatalysis for the silver deposition.[26] Accordingly, the photoreduction of guanine bases of DNAs should play a crucial role in the photocatalytic silver deposition reactions aforementioned. Moreover, Fig. 7D exhibits that the developed colorimetric method can present good detection reproducibility in sensing DNA targets. Therefore, the microwells array-based colorimetric strategy by the photocatalytic silver deposition could allow for the detection of wild DNA targets in blood with high detection sensitivity and selectivity. In particular, it can also allow for the quantification of mutant levels of targeting anthrax DNAs. Besides, the quality Z' factor of the developed colorimetric method was evaluated to be about 0.552, which was calculated using the control data according to the equation reported previously,[29] showing a favorable overall assay quality. Therefore, the developed colorimetric strategy may promise wide applications for the analysis of anthrax DNAs in practical samples.

Conclusions

In summary, a high-throughput, sensitive, and selective colorimetric analysis strategy has been successfully developed using a wettable microwells array for probing guanine base-containing anthrax DNAs in blood, alternatively based on the silver deposition amplified by the synergic combination of TiO_2 photocatalysis and guanine photoreduction. The so developed colorimetric array can possess some outstanding advantages over the common detection methods for DNAs. First, the so-fabricated microwells array with the wettability profile could not only help to obtain condensing-enrichment from sample droplets, but also depress any possible crossover contaminations in-between the sample droplets. Importantly, a highly dense microwells array would thus be obtained toward the high-throughput analysis of multiple samples. Second, the synergic combination of the photocatalysis of TiO_2 and the photoreduction of guanines of targeting DNAs could achieve dramatically amplified silver deposition so as to ensure the highly sensitive detection of DNAs. Third, the DA coatings on TiO_2 nanocatalysts could endow them with tunable photocatalytic responses to visible light, in addition to facilitating the covalent loading of DNA capture probes. Fourth, the use of Exo I to digest the unhybridized ssDNA probes can facilitate the highly selective detection of anthrax DNAs. Finally, the developed microwells array-based colorimetric strategy could not only allow for the detection of guanine-containing anthrax DNAs with high sensitivity and selectivity, but also enable the identification of the single-base and double-base mutation DNAs. Therefore, the developed visualized colorimetric method with a wettable microwells array holds great promise for wide applications in the clinical laboratory for the early diagnosis and the screening of exposure to anthrax. In addition, such a silver deposition amplification strategy by the synergic TiO_2 photocatalysis and guanine photoreduction under visible light may open a new door towards the design of various ultrasensitive analyses in the biomedical, food, and environmental fields.

Conflicts of interest

There are no conflicts to declare.

Acknowledgements

This work was supported by the National Natural Science Foundation of China (No. 21675099, 21375075, and 21601106), and Major Basic Research Program of the Natural Science Foundation of Shandong Province, P. R. China (ZR2018ZC0129).

Notes and references

1 L. P. Xu, Y. Chen, G. Yang, W. Shi, B. Dai, G. Li, Y. Cao, Y. Wen, X. Zhang and S. Wang, *Adv. Mater.*, 2015, **27**, 6878–6884.
2 X. M. Shi, G. C. Fan, X. Tang, Q. Shen and J. J. Zhu, *Biosens. Bioelectron.*, 2018, **109**, 190–196.
3 Y. Zhang, B. Li, H. Ma, L. Zhang and Y. Zheng, *Biosens. Bioelectron.*, 2016, **85**, 287–293.
4 K. C. Addanki, M. Sheraz, K. Knight, K. Williams, D. G. Pace and O. Bagasra, *Indian J. Med. Microbiol.*, 2011, **29**, 372–378.
5 J. Jiang, B. L. Pentelute, R. J. Collier and Z. H. Zhou, *Nature*, 2015, **521**, 545–549.

6 B. C. Bennett, H. Xu, R. F. Simmerman, R. E. Lee and C. G. Dealwis, *J. Med. Chem.*, 2007, **50**, 4374–4381.
7 T. A. Taton, *Science*, 2000, **289**, 1757–1760.
8 J. M. Nam, S. I. Stoeva and C. A. Mirkin, *J. Am. Chem. Soc.*, 2004, **126**, 5932–5933.
9 N. Zhang and D. H. Appella, *J. Am. Chem. Soc.*, 2007, **129**, 8424–8425.
10 H. Wang, L. Zhang, Y. Jiang, L. Chen, Z. Duan, X. Lv and S. Zhu, *Sens. Actuators, B*, 2018, **261**, 441–450.
11 M. Castoldi, S. Schmidt, V. Benes, M. W. Hentze and M. U. Muckenthaler, *Nat. Protoc.*, 2008, **3**, 321–329.
12 A. W. Wark, H. J. Lee and R. M. Corn, *Angew. Chem., Int. Ed.*, 2008, **47**, 644–652.
13 S. Roy, J. H. Soh and Z. Gao, *Lab Chip*, 2011, **11**, 1886–1894.
14 S. Fang, H. J. Lee, A. W. Wark and R. M. Corn, *J. Am. Chem. Soc.*, 2006, **128**, 14044–14046.
15 W. Li and K. Ruan, *Anal. Bioanal. Chem.*, 2009, **394**, 1117–1124.
16 H. Dong, J. Lei, L. Ding, Y. Wen, H. Ju and X. Zhang, *Chem. Rev.*, 2013, **113**, 6207–6233.
17 S. Li, R. Li, M. Dong, L. Zhang, Y. Jiang, L. Chen, W. Qi and H. Wang, *Sens. Actuators, B*, 2016, **222**, 198–204.
18 X. Zhou, S. Xia, Z. Lu, Y. Tian, Y. Yan and J. Zhu, *J. Am. Chem. Soc.*, 2010, **132**, 6932–6934.
19 Y. Si, Z. Sun, N. Zhang, W. Qi, S. Li, L. Chen and H. Wang, *Anal. Chem.*, 2014, **86**, 10406–10414.
20 R. Li, S. Li, M. Dong, L. Zhang, Y. Qiao, Y. Jiang, W. Qi and H. Wang, *Chem. Commun.*, 2015, **51**, 16131–16134.
21 J. Liu, L. de la Garza, L. Zhang, N. M. Dimitrijevic, X. Zuo, D. M. Tiede and T. Rajh, *Chem. Phys.*, 2007, **339**, 154–163.
22 J. M. Rehm, G. L. McLendon, Y. Nagasawa, K. Yoshihara, J. Moser and M. Grätzel, *J. Phys. Chem.*, 1996, **100**, 9577–9578.
23 M. Cargnello, T. R. Gordon and C. B. Murray, *Chem. Rev.*, 2014, **114**, 9319–9345.
24 L. Feng, M. Liu, H. Liu, C. Fan, Y. Cai, L. Chen, M. Zhao, S. Chu and H. Wang, *ACS Appl. Mater. Interfaces*, 2018, **10**, 23647–23656.
25 T. Rajh, Z. Saponjic, J. Liu, N. M. Dimitrijevic, N. F. Scherer, M. Vega-Arroyo, P. Zapol, L. A. Curtiss and M. C. Thurnauer, *Nano Lett.*, 2004, **4**, 1017–1023.
26 T. Rajh, L. X. Chen, K. Lukas, T. Liu, M. C. Thurnauer and D. M. Tiede, *J. Phys. Chem. B*, 2002, **106**, 10543–10552.
27 R. Das, A. K. Goel, M. K. Sharma and S. Upadhyay, *Biosens. Bioelectron.*, 2015, **74**, 939–946.
28 Z. Liu and X. Su, *Anal. Chim. Acta*, 2016, **942**, 86–95.
29 J. H. Zhang, T. D. Chung and K. R. Oldenburg, *J. Biomol. Screening*, 1999, **4**, 67–73.

